Volume 57(6): 523–529, 2009
Journal of Histochemistry & Cytochemistry
http://www.jhc.org

ARTICLE

Tight Junction Proteins in Human Schwann Cell Autotypic Junctions

Maria H. Alanne, Kati Pummi, Anthony M. Heape, Reidar Grènman, Juha Peltonen, and Sirkku Peltonen

Department of Anatomy, Institute of Biomedicine, University of Turku, Turku, Finland (MHA,JP); Department of Dermatology (KP,SP) and Department of Otorhinolaryngology-Head and Neck Surgery (RG), University of Turku and Turku University Central Hospital, Turku, Finland; and Department of Anatomy and Cell Biology, Institute of Biomedicine, University of Oulu, Oulu, Finland (AMH)

SUMMARY Tight junctions (TJs) form physical barriers in various tissues and regulate paracellular transport of ions, water, and molecules. Myelinating Schwann cells form highly organized structures, including compact myelin, nodes of Ranvier, paranodal regions, Schmidt-Lanterman incisures, periaxonal cytoplasmic collars, and mesaxons. Autotypic TJs are formed in non-compacted myelin compartments between adjacent membrane lamellae of the same Schwann cell. Using indirect immunofluorescence and RT-PCR, we analyzed the expression of adherens junction (E-cadherin) and TJ [claudins, zonula occludens (ZO)-1, occludin] components in human peripheral nerve endoneurium, showing clear differences with published rodent profiles. Adult nerve paranodal regions contained E-cadherin, claudin-1, claudin-2, and ZO-1. Schmidt-Lanterman incisures contained E-cadherin, claudin-1, claudin-2, claudin-3, claudin-5, ZO-1, and occludin. Mesaxons contained E-cadherin, claudin-1, claudin-2, claudin-3, ZO-1, and occludin. None of the proteins studied were associated with nodal inter-Schwann cell junctions. Fetal nerve expression of claudin-1, claudin-3, ZO-1, and occludin was predominantly punctate, with a mesaxonal labeling pattern, but paranodal (ZO-1, claudin-3) and Schmidt-Lanterman incisure (claudins-1 and -3) expression profiles typical of compact myelin were visible by gestational week 37. The clear differences observed between human and published rodent nerve profiles emphasize the importance of human studies when translating the results of animal models to human diseases.

(J Histochem Cytochem 57:523–529, 2009)

KEY WORDS
claudin
fetal
human
occludin
peripheral nerve
Schwann cell
tight junction
zonula occludens

PERIPHERAL AXONS are isolated from the surrounding non-nervous tissues by a triple layer of collagen-based connective tissue, including the outermost epineurial layer, that surrounds the whole nerve, the perineurium, which surrounds nerve fascicles, and the innermost endoneurial layer that surrounds individual nerve fibers, and by a Schwann cell sheath. In adults, the Schwann cells form either a myelin sheath or an amyelin sheath. Myelinating Schwann cells wrap around the axon, forming highly organized, compacted, and non-compacted, multilamellar membrane structures. The non-compact structures include the paranodal loop regions, the Schmidt-Lanterman incisures, the periaxonal cytoplasmic collar, and the inner and outer mesaxons. At the nodes of Ranvier, interdigitations of the plasma membranes of adjacent Schwann cells assure the continuity of the Schwann cell sheath along the whole length of the axon, while a continuous, Schwann cell–derived basal lamina forms a permeable boundary between the endoneurial connective tissue layer and the Schwann cell myelin sheath (Thomas 1963).

Perineurial cells of the perineurium form a selective diffusion barrier between the endoneurium and the epineurium (Thomas 1963; Jaakkola et al. 1993; Pummi et al. 2004), and we have previously shown that the tight junction (TJ) proteins zonula occludens (ZO)-1, occludin, claudin-1, and claudin-3 all contribute to the formation of this perineurial diffusion barrier in human

Correspondence to: Sirkku Peltonen, Department of Dermatology, University of Turku, 20520 Turku, Finland. E-mail: sirkku.peltonen@tyks.fi

Received for publication May 6, 2008; accepted January 7, 2009 [DOI: 10.1369/jhc.2009.951681].

0022-1554/09/$3.30

peripheral nerves (Pummi et al. 2004). In epithelia and endothelia, TJs form physical barriers and regulate the paracellular transport of ions, water, and other small molecules by discriminating sizes and charges (Anderson 2001; Hartsock and Nelson 2008).

Several types of junctional specializations, including tight, gap, and adherens junctions, participate in the adhesion of the apposed membrane lamellae in myelinating Schwann cells (Poliak et al. 2002). These junction types are ubiquitous in epithelial tissues, where they are typically formed between neighboring epithelial cells. Because of the fact that, in myelinating Schwann cells, they are formed between membrane lamellae of the same cell, they have been defined as autotypic junctions.

The TJs of epithelial and endothelial cells consist of several adhesion molecules, including ZO-1, -2, and -3, occludin, claudins, and junctional adhesion molecules (Hartsock and Nelson 2008). Occludin, which has four transmembrane domains, two extracellular loops, and three cytoplasmic domains, is capable of binding directly to membrane-associated guanylate kinases (MAGUK), such as ZO-1 (Hartsock and Nelson 2008). Occludin also associates directly with claudins but cannot constitute TJs by itself (Balda and Matter 2000; Anderson 2001). Claudins are integral membrane proteins with four transmembrane domains (Furuse et al. 1998), and they bind homotypically to the same claudin types or heterotypically to different claudin types (Furuse et al. 1999). The identification of 24 claudin types suggests that each claudin has a specific role and function in different tissues (Hartsock and Nelson 2008). In their comprehensive study of TJ protein expression in rodent nerves, Poliak et al. (2002) showed that claudins 1, 2, and 5 are located at the nodes of Ranvier, and in the paranodal regions, Schmidt-Lanterman incisures, and mesaxons of rat sciatic nerve. To our knowledge, TJ protein expression profiles in adult and developing human nerve have not yet been analyzed.

In this study, we extended our previous study of the human peripheral nerve perineurium (Pummi et al. 2004) to Schwann cell autotypic junctions. To determine the detailed localization of claudins, occludin, and ZO-1 in the Schwann cell sheath, we double-labeled fetal and adult human auricular and sciatic nerve teased fiber and frozen section preparations for TJ components, E-cadherin, and various well-known biomarker proteins, including Na^+ channel (for nodes of Ranvier), S-100 (for Schwann cells), type IV collagen (for basal lamina), and class III tubulin (Tuj1, for axons). The expression of claudins 1–11 and 19 was also analyzed at the mRNA level using RT-PCR. The results show clear differences between the expression profiles of claudins in human peripheral nerves and those reported for rodents.

Materials and Methods

Tissue Samples

Tissue samples were obtained with the appropriate informed consent and approval of the Joint Ethical Committee of the Turku University Hospital and the University of Turku, Turku, Finland.

Adult sciatic nerve samples, taken during autopsies performed at the Department of Pathology, Turku University Hospital, Turku, Finland, were from healthy 16-, 21-, 39-, and 40-year-old men who had died in accidents. Sciatic nerve samples from four fetuses were removed during autopsies performed at the Department of Pathology, Turku University Hospital, within 2 days of spontaneous miscarriage after premature labor after 19, 23, 26, and 37 weeks of gestation. The autopsies showed no macroscopic or chromosomal abnormalities. Great auricular nerve samples (~3 cm in length) were removed from four patients (57–75 years of age) for surgical reasons encountered in the course of parotidectomies performed in the Department of Otorhinolaryngology-Head and Neck Surgery, Turku University.

Antibodies

The following primary antibodies were used: rabbit polyclonal antibodies to human claudin-1 (51-9000; concentration 0.25 mg/ml; working dilution 1:100), claudin-2 (51-6100; 0.25 mg/ml; 1:100), claudin-3 (34-1700; 0.25 mg/ml; 1:100), claudin-4 (32-9400; 0.5 mg/ml; 1:100), claudin-5 (34-1600; 0.25 mg/ml; 1:100), claudin-11 (36-4500; 0.25 mg/ml; 1:100), and occludin (71-1500; 0.25 mg/ml; 1:100), and to cow S-100 (18-0046; 167 mg/ml; 1;100), all from Zymed Laboratories (South San Francisco, CA). The use of these polyclonal antibodies has been described previously (Nakajima et al. 1982; Bronstein et al. 1997; Pummi et al. 2004; Peltonen et al. 2007). The following mouse monoclonal antibodies were used: human claudin-5 (35-2500; 0.5 mg/ml; 1:100; Zymed), type IV collagen (C1926; 6 mg/ml; 1:300; Sigma-Aldrich, St. Louis, MO), E-cadherin (33-4000; 0.5 mg/ml; 1:100; Zymed), ZO-1 (33-9100; 0.5 mg/ml; 1:100; Zymed), occludin (33-1500; 0.5 mg/ml; 1:100; Zymed), pan Na^+ channel (S8809; 1.1 mg/ml; 1:100; Sigma-Aldrich), and Class III β-tubulin (Tuj1; MMS-435P; 1 mg/ml; 1:100; Nordic BioSite, Täby, Sweden). The use of these monoclonal antibodies has been described previously (Rasband et al. 1999; Pummi et al. 2004,2006; Peltonen et al. 2007; Jouhilahti et al. 2008). Alexa Fluor 488 (A11029; 2.0 mg/ml; 1:100) and Alexa Fluor 568 (A11011; 2.0 mg/ml; 1:300; Invitrogen, Eugene, OR) were used as secondary antibodies. Hoechst nuclear stain (H3570, 10.0 mg/ml; 1:15,000; Invitrogen) was used for the fluorescent labeling of cell nuclei.

Preparation of Teased Nerve Fibers

Great auricular nerve samples were immediately immersed in sterile PBS at room temperature. The samples were brought to the laboratory and, within 10 min after the removal of the nerve, the tissue was fixed in 10% formaldehyde for 15 min. The nerve samples were washed with PBS, cut into 2- to 3-mm pieces, placed in double-distilled water, and teased immediately. Connective tissue and fat tissue were removed under a preparation microscope, and the epineurium and perineurium were opened with fine forceps. The endoneurium was transferred onto silanated glass slides, and Schwann cell-axon units were teased with fine needles to separate the fibers. After air drying, the samples were postfixed and permeabilized in methyl alcohol at −20C for 20 min. Slides were blocked for 30 min with PBS containing 1% BSA and 0.1% Triton-X-100. Samples were treated with the same antibodies and protocol as the frozen sections (see below).

Indirect Immunofluorescence Labeling

Frozen nerve samples were cut into 7-μm cryosections on silanated glass slides and fixed in 100% methyl alcohol at −20C for 10 min. To prevent nonspecific binding, the samples were preincubated in 1% BSA-PBS for 30 min. Antibodies were diluted in 1% BSA-PBS and incubated on the samples for 18–22 hr at 4C. After five 5-min washes in PBS, the samples were incubated for 2 hr, at 20C, with secondary antibodies diluted in 1% BSA-PBS and Hoechst nuclear stain. The labeled samples were washed in PBS and mounted with Glycergel (Dako; Glostrup, Denmark). In control immunoreactions, primary antibodies were replaced with 1% BSA-PBS.

RNA Isolation and RT-PCR

RNA was isolated from the sciatic nerves of 19- and 26-week-old fetal and adult great auricular nerves as follows. Three-mm pieces of the nerve were immediately submerged in RNAlater RNA Stabilization Reagent (76104; Qiagen, Valencia, CA). RNA was isolated using the RNeasy Mini Kit (74104; Qiagen) according to the protocol provided by the manufacturer. The RNA was reverse-transcribed into single-strand cDNA in a 20-μl reaction containing 200 units of SuperScript II Reverse Transcriptase (18064-022; Invitrogen, Carlsbad, CA), 1 μM of each of the four deoxynucleotides, random hexamers (C1181; Promega, San Luis Obispo, CA), 20 units of RNasin (N2111; Promega), and 0.01 M dithiothreitol in the first-strand buffer. The reaction was incubated at 42C according to the first-strand synthesis protocol provided by the manufacturer. The cDNAs yielded by RT reactions were used as templates for PCR amplification. PCR reactions for claudins 1–11 and GAPDH were performed using a MultiGene-12 RT-PCR profiling Kit (PH-083B; SuperArray Bioscience, Frederick, MD) detecting claudins 1–11, according to the protocol provided by the manufacturer. PCR reactions for claudin 19 were performed as described by Lee et al. (2006), using claudin 19 primers (sense primer: 5′-AATTTGGCCCAGCCCTGTTCGTGG-3′; anti-sense primer: 5′-GATTGGATGTGACCGTCCAGGGCG-3′). The product size was 290 bp. In brief, 2 μl cDNA was mixed with 18 μl PCR reaction buffer containing 5× Phusion HF buffer (Finnzymes Oy; Espoo, Finland), 200 nM primers, 200 μM dNTPs, and 0.4 U of Phusion Hot Start DNA Polymerase (Finnzymes Oy). PCR conditions were 30 cycles of 94C for 40 sec, 64C for 30 sec, and 72C for 40 sec, with a final extension at 72C for 10 min.

Microscopy

Confocal laser scanning microscopy was carried out using a Zeiss LSM 510 META confocal microscope equipped with argon-ion and helium-neon lasers (Zeiss; Jena, Germany) and LSM 3.0 software. The objectives were ×40 (oil immersion, numeric aperture 1,3), ×63 (oil immersion, numeric aperture 1,4), and ×100 (oil immersion, numeric aperture 1,4). For excitation, the 405-nm line was used for Hoechst, the 488-nm line for Alexa Fluor 488, and the 543-nm line for Alexa Fluor 568. The beam path for Alexa 488 Fluor contained a 488-nm main dichroic mirror and a 500-550IR bandpass filter. The beam path for Alexa Fluor 568 contained a 543-nm main dichroic mirror and a 565-615IR filter for detection of the fluorescence emissions. The resolution of original images was 2048 × 2048 pixels, and images were saved in tif format.

Results

Adult nerves

Immunofluorescence confocal microscopy and RT-PCR analyses of human sciatic and great auricular nerves were performed to determine the adult and fetal protein and mRNA expression profiles of junctional components in human myelinating Schwann cells. Claudin-1 was readily detectable in Schmidt-Lanterman incisures and outer mesaxons, where it colocalized with E-cadherin (Figures 1A–1C); in paranodal regions, where it colocalized with ZO-1; and in periaxonal membranes (Figures 1E and 1F).

Like claudin-1, claudin-2 was also clearly expressed with E-cadherin in Schmidt-Lanterman incisures (Figures 1G and 1H) and in paranodal regions (Figure 1H, inset), but also in the periaxonal cytoplasmic collar, from which E-cadherin was absent. On the other hand, contrasting with both claudin-1 and E-cadherin, claudin-2 expression was barely detectable in the outer membranes of the sheath.

Claudin-3 (Figure 1I) was also clearly detected in Schmidt-Lanterman incisures and, to a lesser extent, in

mesaxonal membranes, but was absent from the paranodal and nodal regions, whereas claudin-5 was observed only in Schmidt-Lanterman incisures (Figure 1J). Claudin-4 and claudin-11 were not detected at the protein level.

Labeling for occludin (Figure 1D) was generally sparse, punctate, and weak, with a mesaxonal-like distribution and occasional labeling of Schmidt-Lanterman incisures (Figure 1D inset).

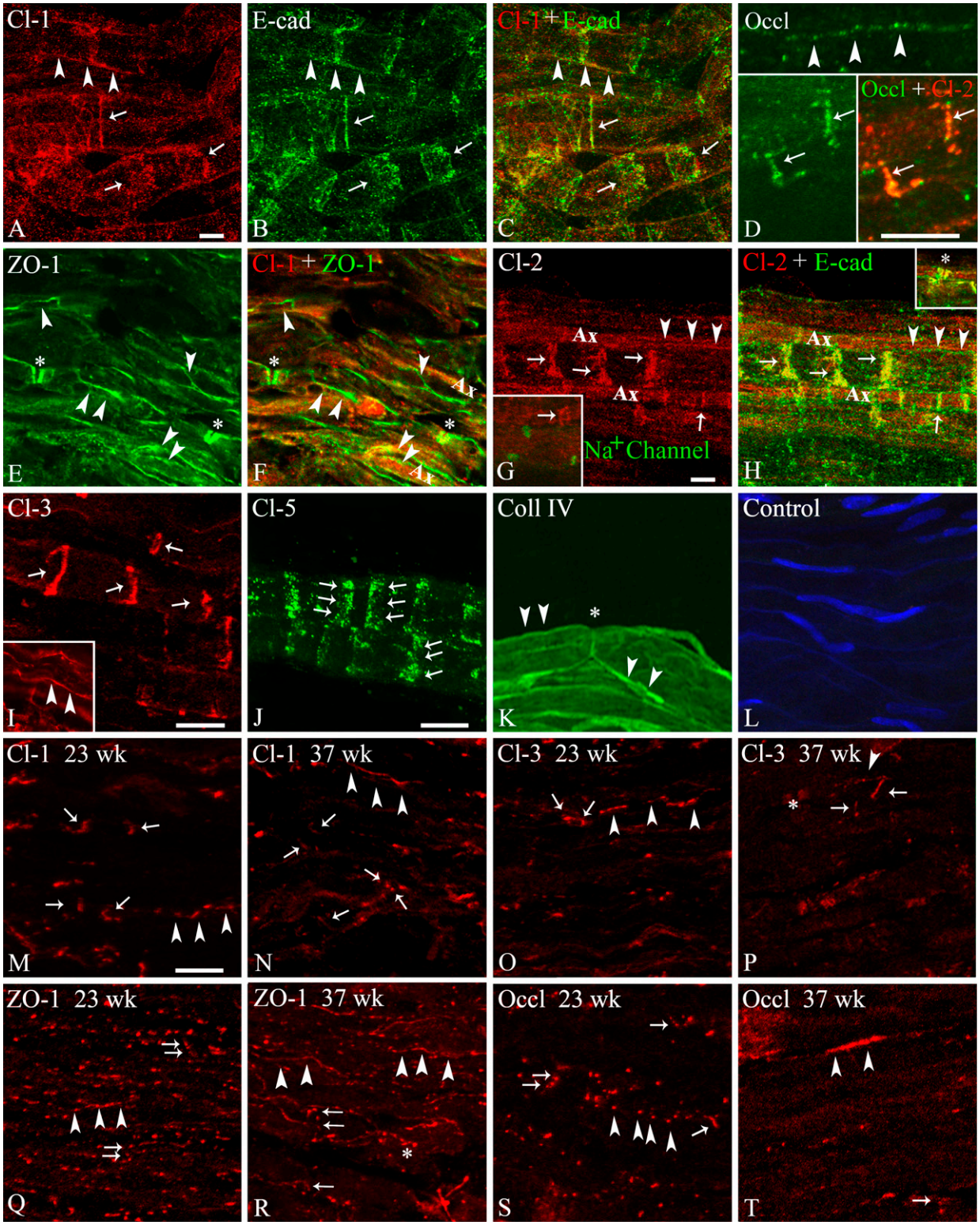

The results of the immunofluorescence confocal microscopy analyses of the adult nerves are summarized in Table 1. Paranodal areas contained claudin-1, claudin-2, E-cadherin, and ZO-1. Schmidt-Lanterman incisures contained E-cadherin, ZO-1, claudin-1, claudin-2, claudin-3 claudin-5, and occludin. Claudin-1, claudin-2, claudin-3, ZO-1, occludin, and E-cadherin were localized in mesaxons. None of the junctional proteins were detected in the regions directly adjacent to the nodes of Ranvier where they could participate in the maintenance of the plasmalemmal interdigitations between adjacent Schwann cells along the axon.

RT-PCR analysis of RNA isolated from adult great auricular nerves showed a strong expression of claudin-1 mRNA, whereas claudin-2, -6, -7, -8, -9, and -11 mRNAs were expressed at similar moderate levels, and claudin-3 and -4 were expressed at very low levels. Claudin-5 and claudin-10 (Figure 2) mRNAs were not detectable. RT-PCR showed no mRNA expression for claudin-19 in adult great auricular nerve or in fetal sciatic nerves at 19 and 26 weeks of gestation (data not shown).

Developing Nerves

Immunofluorescence confocal microscopy of cryosectioned sciatic nerves from 23- and 37-week fetuses showed the expression of claudin-1 (Figures 1M and 1N), claudin-3 (Figures 1O and 1P), ZO-1 (Figures 1Q and 1R), and occludin (Figures 1S and 1T). At 23 weeks, all four antigens exhibited a predominantly punctate labeling pattern arranged linearly throughout the endoneurium, suggestive of a mesaxonal localization. At week 37, the linear, mesaxonal expression of all four proteins was more evident, and a typical paranodal expression of ZO-1 and claudin-3 was clearly visible. Occasional Schmidt-Lanterman incisures could also be identified in the cases of claudins-1 and 3, particularly at 37 weeks, indicating that myelin compaction, although still in its very early stages, was underway.

Discussion

Studies of Schwann cell TJs have, thus far, been carried out almost exclusively using rodent tissues. In this study, we provided the first demonstration of the expression of both TJ and adherens junction proteins in the non-compacted membrane compartments of developing and adult human Schwann cells (Figure 1). Among the latter, Schmidt-Lanterman incisures of adult nerves contained the adherens junction protein E-cadherin and the TJ proteins claudins-1, -2, -3, and -5, ZO-1, and occasionally occludin, whereas paranodal regions also contained E-cadherin, claudins-1 and -2, and ZO-1, but not claudin-3 or -5 or occludin. E-cadherin, claudins-1 and -3, ZO-1, and occludin were also expressed in the abaxonal (outer) mesaxon membranes of the sheath, whereas mesaxonal expression of claudin-2 was mostly limited to the adaxonal (inner) compartments, in which claudin-1, although present, was generally less abundant.

Our results differ somewhat from those reported for rodent peripheral nerves with respect to the expression of claudins-2, -3, and -5. Poliak et al. (2002) showed that claudin-2 participates in forming TJs between the inter-Schwann cell microvilli located around the nodes of Ranvier of mouse sciatic nerves. Although claudin-2 was present in the paranodal membrane compartments of human nerves, we could not detect any of the claudins studied here in the nodal area, where they could participate in the stabilization of the plasmalemmal interdigitations linking adjacent

Figure 1 Immunofluorescence confocal microscopy of adherens and tight junction components in human adult great auricular nerve (**A–C,G, H,J,K**) and sciatic nerve (**D–F,I,L**) and fetal sciatic nerve at gestational ages of 23 (**M,O,Q,S**) and 37 weeks (**N,P,R,T**). All great auricular nerve samples are teased endoneurial fiber, and all sciatic nerve samples are longitudinal endoneurial cryosections, prepared as described in the Materials and Methods section. In all panels, arrows indicate Schmidt-Lanterman incisures, arrowheads indicate mesaxons, asterisks denote paranodal regions, and Ax indicates axons. Adult nerves (**A–L**). (**A–C**) Double labeling for (**A**) claudin-1 (Cl-1: red) and (**B**) E-cadherin (E-cad: green) in adult great auricular nerve showing colocalization (**C**: yellow) in outer mesaxonal membranes and Schmidt-Lanterman incisures. (**D**) Double labeling for claudin-2 (Cl-1: red) and occludin (green) in adult sciatic nerve showing punctate occludin expression in mesaxons (top) and colocalization (bottom right: yellow) in outer Schmidt-Lanterman incisures. (**E,F**) Double labeling for claudin-1 (Cl-1: red) and zonula occludens (ZO)-1 (**E**: green) in adult sciatic nerve showing colocalization (**F**: yellow) in paranodal regions and partial colocalization in mesaxonal membranes. (**G,H**) Double labeling for (**G**) claudin-2 (Cl-2: red) and E-cadherin (E-cad: green) in adult great auricular nerve showing periaxonal (mesaxonal) claudin-2 expression and colocalization (**C**: yellow) in Schmidt-Lanterman incisures and paranodal regions (inset in **H**). The inset in **G** shows nodes of Ranvier labeled with antibodies for the pan-Na^+ channel (green). (**I**) Mono-labeling for claudin-3 (Cl-3: red) showing expression in Schmidt-Lanterman incisures and mesaxonal membranes (inset) of sciatic nerve. (**J**) Mono-labeling for claudin-5 (Cl-5: green) showing expression in Schmidt-Lanterman incisures of great auricular nerve. (**K**) Mono-labeling for type IV collagen (Coll IV: green) showing the great auricular nerve Schwann cell–derived basal lamina that surrounds each myelin segment. (**L**) Control labeling of sciatic nerve endoneurium using both secondary antibodies, without primary antibodies. Nuclei are visualized with Hoechst nuclear stain (blue). Fetal nerves (**M–T**). (**M,N**) Claudin-1 (Cl-1) expression at gestational weeks 23 (**M**) and 37 (**N**) showing the sparse, punctate labeling of mesaxonal membranes and Schmidt-Lanterman incisures. (**O,P**) Claudin-3 (Cl-3) expression at gestational weeks 23 (**O**) and 37 (**P**) showing the sparse, punctate labeling of mesaxonal membranes, rare Schmidt-Lanterman incisures and, at 37 weeks, paranodal regions. (**Q,R**) ZO-1 expression at gestational weeks 23 (**Q**) and 37 (**R**) showing the punctate labeling of mesaxonal membranes throughout the endoneurium, rare Schmidt-Lanterman incisures, and, at 37 weeks, paranodal regions. (**S,T**) Occludin (Occl) expression at gestational weeks 23 (**S**) and 37 (**T**) showing the sparse, punctate labeling of mesaxonal membranes and rare Schmidt-Lanterman incisures. Bar = 10 μm.

Table 1 Expression of claudin, occludin, zonula occludens-1, and E-cadherin in adult human and rodent[a,b,c] endoneurium

	Paranodal area	Schmidt-Lanterman incisure	Mesaxon	Node of Ranvier
Proteins	Human/rodent[a]	Human/rodent	Human/rodent	Human/rodent
Claudin-1	+/+	+/−	+/+	−/−
Claudin-2	+/−	+/−	+/−	−/+
Claudin-3	−/−[d]	+/−	+/−	−/−
Claudin-5	−/−	+/+	−/−	−/−
Occludin	+[e]/−[b]	+[e]/−[b]	+/−[b]	−/−[b]
Zonula occludens-1	+/+	+/+	+/+	−/−
E-cadherin	+/+[c]	+/+[c]	+/+[c]	−/−[c]

[a]Poliak et al. 2002.
[b]Nagaoka et al. 1999.
[c]Fannon et al. 1995.
[d]Claudin-3 was detected in paranodal areas of human fetal nerves at 37 weeks.
[e]Occludin labeling in Schmidt-Lanterman incisures and paranodal areas of fetal nerves could not be distinguished from each other.

Schwann cell sheaths along the axon. It is possible that other components of the 24-member claudin family not studied here could fulfill this function. Claudin-3 protein expression was not detected in the mouse sciatic nerve (Poliak et al. 2002), whereas we showed that, in human nerves, claudin-3 is present in both Schmidt-Lanterman incisures and mesaxons.

The differences observed between mouse and human TJ protein expression profiles extend also to the mRNA expression profiles. Indeed, whereas Poliak et al. (2002) studied the expression of mRNA for claudins 1–16 and detected the expression of claudin-1, -2, -5, -10, and -15 in the mouse sciatic nerve, we studied the mRNA expression of claudins 1–11 and 19 in human great auricular nerves and detected the expression of claudin-1, -2, -3, -4, -6, -7, -8, -9, and -11. The expression of claudin-1, -2, and -3 in the human nerves was in concordance with the expression detected at the protein level. In contrast, although claudin-5 protein was clearly expressed in Schmidt-Lanterman incisures, its mRNA was not detected by PCR, suggesting a very low turnover rate for this protein in the myelin sheath. On the other hand, claudin-4 and -11, although detected in the RT-PCR analyses, were not detected at the protein level in this study or in fetal or adult endo- or perineurium, suggesting that the mRNA is not translated in human peripheral nerves. This is in accordance with previous studies on rodents showing that claudin-11 is expressed in the central nervous system, whereas the peripheral nervous system lacks claudin-11 (Gow et al. 1999; Morita et al. 1999; Miyamoto et al. 2005). We did not analyze the expression of claudins 6–10 and 19 at the protein level in this study.

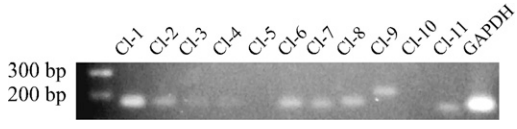

Figure 2 RT-PCR for claudins 1–11 and GAPDH in human adult great auricular nerve. Expression of mRNAs for claudins 1–4, claudins 6–9, claudin-11, and GAPDH is shown as 160- to 210-bp fragments.

The biological significance of these differences between rodents and human remains to be elucidated, but our observations underscore the necessity for caution when extrapolating results obtained using mouse models to a human context. For example, because claudin-19–deficient mice showed different nerve conduction characteristics in sciatic nerve compared with control mice (Miyamoto et al. 2005), it would be tempting to attribute a role for claudin-19 in human nerve conduction. However, the expression of claudin-19 in human nerves has not yet been reported. The availability of numerous bioengineered and spontaneous mutant mice presenting phenotypes that mimic human diseases, including peripheral nervous system ailments, makes it tempting to use these animals as model systems for studying these diseases. Our results showing that there are slight, but significant, differences in the expression patterns between the species emphasize the importance of performing confirmatory human studies to establish the relevance and validation of the animal models. Claudins may indeed have an impact on axonal function in the peripheral nerves, but humans and rodents may use different claudins for the same functions.

The localization of the TJ components claudin and ZO-1 in non-compact myelin is in accordance with previous ultrastructural studies that showed TJ strands in the inner and outer mesaxons, paranodal loops, and Schmidt-Lanterman incisures (Inokuchi and Higashi 1980; Shinowara et al. 1980; Stolinski and Breathnach 1982). Similarly, adherens junctions containing E-cadherin have been shown in the same specific non-compact myelin areas (Fannon et al. 1995; Poliak et al. 2002). Because the junctions apparently have features of both tight and adherens junctions, it has been discussed whether these autotypic junctions should be called TJs or adherens junctions (Fannon et al. 1995). In this study, all claudins detected at the protein level showed colocalization with ZO-1 and E-cadherin. The combination of TJ proteins would thus allow formation of

structural autotypic junctions with a regulatory role in ion permeability. The presence of E-cadherin in the same regions would provide an additional link from the plasma membrane to the actin cytoskeleton, increasing mechanical strength.

In general, TJs have two main functions: they act as selective permeability barriers and as intramembranous fences that prevent the mixing of membrane proteins between specific membrane domains (Hartsock and Nelson 2008). The function of autotypic TJs in myelinating Schwann cells is not entirely clear, but, considering the location of claudins in Schwann cells, both of the principal functions of TJs can be considered to be necessary for stabilizing intermembrane adhesion and for segregating the non-compacted myelin membrane domains from those of the compact myelin. Restricting the diffusion of axonal proteins at the paranodal junction may also be important in maintaining specialized myelin compartments. The relevance of these junctions to the maintenance of myelin integrity, saltatory conduction, and different peripheral neuropathies remains to be elucidated.

We previously studied TJ protein expression in developing human peripheral nerves with special attention to the perineurium (Pummi et al. 2004), showing that the different TJ proteins followed slightly different expression time tables during embryonic development and that the structural diffusion barrier matured late during fetal life. In humans, myelination initiates during the second trimester (Tanaka et al. 1995), although the exact time table may vary from one region of the nervous system to another. In this study, claudin-1, claudin-3, occludin, and ZO-1 antibodies showed punctate labeling with mesaxon-like profiles in the second trimester, and occasional Schmidt-Lanterman incisures and paranodal regions can be distinguished during the third trimester, indicating the formation of immature TJs and the initiation of at least a minimum of myelin compaction by 37 weeks of gestation. This contrasts sharply with the rodent peripheral nerve myelination program, which does not start until after birth.

Literature Cited

Anderson JM (2001) Molecular structure of tight junctions and their role in epithelial transport. News Physiol Sci 16:126–130

Balda M, Matter K (2000) Transmembrane proteins of tight junctions. Semin Cell Dev Biol 11:281–289

Bronstein JM, Micevych PE, Chen KJ (1997) Oligodendrocyte-specific protein (OSP) is a major component of CNS myelin. Neurosci Res 50:713–720

Fannon AM, Sherman DL, Ilyina-Gragerova G, Brophy PJ, Friedrich VL Jr, Colman DR (1995) Novel E-cadherin-mediated adhesion in peripheral nerve: Schwann cell architecture is stabilized by autotypic adherens junctions. J Cell Biol 129:189–202

Furuse M, Sasaki H, Fujimoto K, Tsukita S (1998) A single gene product, claudin-1 or -2, reconstitutes tight junction strands and recruits occludin in fibroblasts. J Cell Biol 143:391–401

Furuse M, Sasaki H, Tsukita S (1999) Manner of interaction of heterogeneous claudin species within and between tight junction strands. J Cell Biol 147:891–903

Gow A, Southwood CM, Li JS, Pariali M, Riordan GP, Brodie SE, Danias J, et al. (1999) CNS myelin and Sertoli cell tight junction strands are absent in Osp/Claudin-11 null mice. Cell 99:649–659

Hartsock A, Nelson WJ (2008) Adherens and tight junctions: structure, function and connections to the actin cytoskeleton. Biochim Biophys Acta 1778:660–669

Inokuchi T, Higashi R (1980) Mesaxonal membrane junction of myelinated nerve in the central and peripheral nervous system. Arch Histol Jpn 43:221–229

Jaakkola S, Savunen O, Halme T, Uitto J, Peltonen J (1993) Basement membranes during development of human nerve: Schwann cells and perineurial cells display marked changes in their expression profiles for laminin subunits and beta 1 and beta 4 integrins. J Neurocytol 22:215–230

Jouhilahti EM, Peltonen S, Peltonen J (2008) Class III {beta}-tubulin is a component of the mitotic spindle in multiple cell types. J Histochem Cytochem 56:1113–1119

Lee NP, Tong MK, Leung PP, Chan VW, Leung S, Tam PC, Chan KW, et al. (2006) Kidney claudin-19: localization in distal tubules and collecting ducts and dysregulation in polycystic renal disease. FEBS Lett 580:923–931

Miyamoto T, Morita K, Takemoto D, Takeuchi K, Kitano Y, Miyakawa T, Nakayama K, et al. (2005) Tight junctions in Schwann cells of peripheral myelinated axons: a lesson from claudin-19-deficient mice. J Cell Biol 169:527–538

Morita K, Furuse M, Fujimoto K, Tsukita S (1999) Claudin multigene family encoding four-transmembrane domain protein components of tight junction strands. Proc Natl Acad Sci USA 96:511–516

Nagaoka T, Oyamada M, Okajima S, Takamatsu T (1999) Differential expression of gap junction proteins connexin26, 32, and 43 in normal and crush-injured rat sciatic nerves. Close relationship between connexin43 and occludin in the perineurium. J Histochem Cytochem 47:937–948

Nakajima T, Watanabe S, Sato Y, Kameya T, Hirota T, Shimosato Y (1982) An immunoperoxidase study of S-100 protein distribution in normal and neoplastic tissues. Am J Surg Pathol 6: 715–727

Peltonen S, Riehokainen J, Pummi K, Peltonen J (2007) Tight junction components occludin, ZO-1, and claudin-1, -4 and -5 in active and healing psoriasis. Br J Dermatol 156:466–472

Poliak S, Matlis S, Ullmer C, Scherer SS, Peles E (2002) Distinct claudins and associated PDZ proteins form different autotypic tight junctions in myelinating Schwann cells. J Cell Biol 159: 361–372

Pummi KP, Aho HJ, Laato MK, Peltonen JT, Peltonen SA (2006) Tight junction proteins and perineurial cells in neurofibromas. J Histochem Cytochem 54:53–61

Pummi KP, Heape AM, Grénman RA, Peltonen JT, Peltonen SA (2004) Tight junction proteins ZO-1, occludin, and claudins in developing and adult human perineurium. J Histochem Cytochem 52:1037–1046

Rasband MN, Peles E, Trimmer JS, Levinson SR, Lux SE, Shrager P (1999) Dependence of nodal sodium channel clustering on paranodal axoglial contact in the developing CNS. J Neurosci 19: 7516–7528

Shinowara NL, Beutel WB, Revel JP (1980) Comparative analysis of junctions in the myelin sheath of central and peripheral axons of fish, amphibians and mammals: a freeze-fracture study using complementary replicas. J Neurocytol 9:15–38

Stolinski C, Breathnach AS (1982) Freeze-fracture replication of mammalian peripheral nerve–a review. J Neurol Sci 57:1–28

Tanaka S, Mito T, Takashima S (1995) Progress of myelination in the human fetal spinal nerve roots, spinal cord and brainstem with myelin basic protein immunohistochemistry. Early Hum Dev 41:49–59

Thomas PK (1963) The connective tissue of peripheral nerve: an electron microscope study. J Anat 97:35–44

The Journal of Histochemistry & Cytochemistry